BED-Vol. 26, 1993 Advances in Bioengineering
ASME 1993

# AMPPULSE THEORY AS THE ETIOLOGY OF ATHEROSCLEROSIS IN BRANCHED VESSELS

Rupak K. Banerjee*, Ph. D.
Young I. Cho, Ph. D.
Kenneth R. Kensey,** M.D.

Department of Mechanical Engineering and Mechanics
Drexel University, Philadelphia, PA 19104

*Fluid Analysis Group, Raytheon,
30th South 17th St., Philadelphia, PA19101

**Kensey Nash Corp., 55E. Uwchlan Ave,
Suite 204, Exton, PA 19341

## ABSTRACT

To validate the 'amppulse' flow as the etiology of atherosclerosis, computer simulation and analysis are presented. Two different pulsatile flows: 'amppulse' and 'less-amppulse' are used to numerically simulate *in-vivo* blood flow. The effect of 'amppulse' and 'less-amppulse' pumping on the injury of endothelial cells is investigated by calculating instantaneous wall shear stresses of a normal 90° femoral artery.

At the proximal and the distal branch apex, the oscillating wall shear stresses calculated from 'amppulse' pulse cycle are found to be substantially greater than those from 'less-amppulse'. The 'amppulse' theory presents the pathological change in wall shear stress magnitude and direction which cause injury to the intima cell layer of the arterial wall. The comparison of results of 'amppulse' and 'less-amppulse' indicate that if one can slightly modify the 'amppulse' to 'less-amppulse', the injury to the arterial branches may be reduced thus slowing the progression of or causing regression of atherosclerosis.

## NOMENCLATURE

- $t$ = time
- $u$ = velocity vector
- $x$ = distance along the main lumen
- $y$ = distance along the branch lumen
- $\eta$ = viscosity
- $\rho$ = density

## INTRODUCTION

A new hypothesis proposes that an amplified protosystolic pulse (called here, 'Amppulse') circulation injures the arterial wall by first over-stretching (thus inducing arteriosclerosis), and then by magnified shear stress on the intima (inducing atherosclerosis). 'Amppulse' circulation is defined as an injury-inducing blood flow caused by the left ventricle that is contracting too vigorously for a particular blood pressure and blood viscosity. 'Amppulse' circulation exists when the excessive work of the heart results in injury to the vascular system. This hypothesis is based on the premise that when the vascular system absorbs damaging forces from 'Amppulse' circulation, it will react in such a way (by thickening, hardening, etc.) as to resist future damage. The present study intends not only to understand and explain this new hypothesis, but also to quantify critical flow parameters in order to suggest a way to retard the progression of the disease.

As seen in the angiogram (Fig. 1), lesions often occur at these branch sites and subsequently, the fluid dynamics of arterial flow and the related mass transport have been implicated to be factors in the genesis of atherosclerotic lesions. The literature review on branch flow has been presented by Banerjee et al. [1993] and hence, has not been repeated here.

Fig. 1 The striking symmetric locations of apparent lesions at branches are shown by arrows. Blood flow is from top to bottom.

The objective of the present study was to numerically calculate temporal and spatial dependent shear stress in a branch junction arterial model in order to understand the effect of 'amppulse' cycle on the flow field at the site-specific lesion formation regions.

## METHODS

The focus of this study is on a branch angle of 90°, which is commonly observed in the downstream portion of the femoral artery (Fig. 1). The ratio of branch to main lumen width $d_b/d_s$ is 0.4. The arterial branch model has upstream and downstream main lumen widths of 0.631 cm and branch width of 0.252 cm which is similar to femoral artery branches of man reported by Cho et al [1985].

This study deals with finite element analysis [FEM] of the time-dependent solution of an incompressible, non-Newtonian model for the selected geometry. The Galerkin formulation (Baker [1983]) using nine nodal quadrilateral elements is applied herein to discretize the continuity and momentum equations, which result in a set of nonlinear algebraic equations of the form

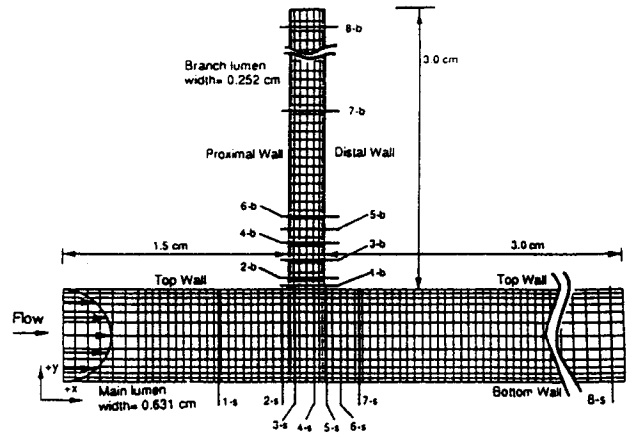


Fig. 2 The mesh plot along with dimension of a 90° branch femoral artery.

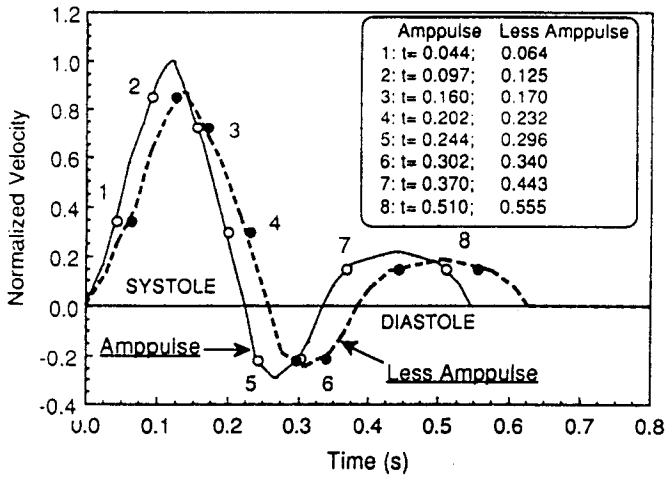


Fig. 3 Normalized form of the *in-vivo* velocity pulse near the core of the femoral artery along a pulse cycle obtained by doppler flow meter. Also shown are the various time steps (No. 1 to No. 8) for which flow data are reported.

$$M\frac{du}{dt} + K(u)\,u = F \qquad (1)$$

where K(u) is the global system matrix developed from the momentum balance, M is the mass matrix, u is the velocity unknown, and F is the forcing function (body forces and boundary conditions). For spatial integration a combination of the successive substitution and quasi-Newton scheme is used whereas for implicit time integration the second order trapezoidal method is adopted.

The mesh plot for the artery is shown in Fig. 2. Spatial variations of shear stress, at various time steps, are obtained at axial wall locations for main and branch lumen. Time histories of wall shear stress at critical wall locations of both main and branched lumens are also presented here.

Two pulsatile velocity cycles are shown in Fig. 3, where 'amppulse' circulation is identified as an elevated protosystolic acceleration of blood flow for a specific blood pressure and blood viscosity. The normalized instantaneous tri-phasic inlet velocity profile ($u/u_{peak}$) has been replotted from the *in-vivo* velocity profile measurement (Risoe and Wille [1978]). The 'amppulse' peak input velocity ($u_{peak}$) is 36.3 cm/sec at t= 0.122 s whereas for 'less-amppulse' case it is 31.6 cm/sec at t= 0.139 s. The normalized tri-phasic inlet velocity profile is used as an instantaneous input for the numerical calculations. Fully developed flows are used as spatial distribution for inlet flows. The selected time steps for flow analysis have been marked from No. 1 to No. 8 in Fig. 3. The no-slip boundary condition has been specified on the rigid arterial wall. At the outlet no boundary condition is specified.

The Carreau model is used where $\lambda$ (characteristics time) = 3.313 s, $n = 0.3568$, $\eta_0 = 0.56$ poise, $\eta_\infty = 0.0345$ poise. Blood with a constant density of 1.05 g/cm$^3$ is used in the calculations. Further detail on numerical procedure and shear stress calculations have been presented by Banerjee et al. [1993] and hence, have not been repeated here.

## RESULTS AND DISCUSSION

This section contains an insight into the difference in shear stress between 'amppulse' and 'less-amppulse' circulations in a 90° human femoral artery. For detail on variation of flow parameters in a 90° human femoral artery Banerjee et. al. [1993] may be refered to.

### WALL SHEAR STRESS -'AMPPULSE' vs 'LESS-AMPPULSE' CIRCULATION

The wall shear stress, for 'amppulse' circulation, which shows a combined effect of the non-Newtonian viscosity and shear rate, is presented in Figs. 4A-4D. At the downstream location of both main and branch lumens the shear stress variation is oscillatory in nature (i.e., arrow #2 in Fig. 4A), due to the tri-phasic nature of the pulse, having values in the range of 16 dynes/cm$^2$ to -12 dynes/cm$^2$. The oscillatory shear stress values vary as the fluid encounters the branch lumen. At t = 0.16 s, i.e., during the decelerating phase of systole, both negative and positive shear stress levels are observed (i.e., arrow #1 for plot No. 3 in Fig. 4A), indicating the existence of a recirculating region at that instant in time. At the top wall near the proximal branch orifice, the shear rate reaches a value of 48 dynes/cm$^2$ at t = 0.097 s (i.e., arrow #1 for plot No. 2 in Fig. 4B) whereas it reaches -6.7 dynes/cm$^2$ at t = 0.202 s, showing a sharp increase in the magnitude of oscillatory shear stress and a shift in a positive direction. Similarly, at the top wall near the distal branch orifice, the shear rate reaches a value of 28.5 dynes/cm$^2$ at t = 0 s (i.e., arrow #2 for plot No. 2 in Fig. 4B) whereas it reaches -6.2 dynes/cm$^2$ at t = 0.243 s. The shear stress for the proximal branch wall near the entry region of branch shows a value of -33.6 dynes/cm$^2$ at t = 0.243 s (i.e., arrow #1 for plot No. 5 in Fig. 4C) indicating a shift in oscillatory shear in a negative direction whereas the distal branch wall shows a value of 45.5 dynes/cm$^2$ (i.e., arrow #1 for plot No. 2 in Fig. 4D), a shift in oscillatory shear in a positive direction.

The wall shear stress for 'less-amppulse' circulation is presented in Figs. 5A-5D. At the downstream location of both the main and branch lumens the value of shear stress oscillates between 13 dynes/cm$^2$ and -8.5 dynes/cm$^2$ (i.e., arrow #2 in Fig. 5A) due to the tri-phasic nature of the pulse. At t = 0.17 s, i.e., during the decelerating phase of systole, only a positive shear stress is observed (i.e., arrow #1 for plot No. 3 in Fig. 5A). At the top wall of the main lumen, near the proximal branch orifice, the shear rate reaches a value of 40 dynes/cm$^2$ at t = 0.125 s (i.e., arrow #1 for plot No. 2 in Fig. 5B) whereas it reaches -5.2 dynes/cm$^2$ at t = 0.232 s, showing an increase in magnitude and a shift in the positive direction of oscillatory shear stress. Similarly, at the top wall near the distal branch orifice, the shear rate reaches a value of 27 dynes/cm$^2$ at t = 0.125 s (i.e., arrow #2 for plot No. 2 in Fig. 5B) whereas it reaches -4.5 dynes/cm$^2$ at t = 0.296 s. The shear stress for the proximal branch wall near the entry region of the branch becomes -24.2 dynes/cm$^2$ at t = 0.296 s (i.e., arrow #1 for plot No. 5 in Fig. 5C), indicating a shift in oscillatory shear in a negative direction whereas the distal wall has a shear stress of 44.13 dynes/cm$^2$ (i.e., arrow #1 for plot No. 2 in Fig. 5D), a shift in oscillatory shear in a positive direction.

Figures 6A-6B show time history shear stress plots for 'amppulse' circulation whereas Figs. 7A-7B show for 'less-amppulse' circulation. For 'amppulse' circulation, at t = 0.104 maximum wall shear stress of 50.9 dynes/cm$^2$ occurs at the top wall of the main lumen located near the proximal branch apex (x = 1.5 cm

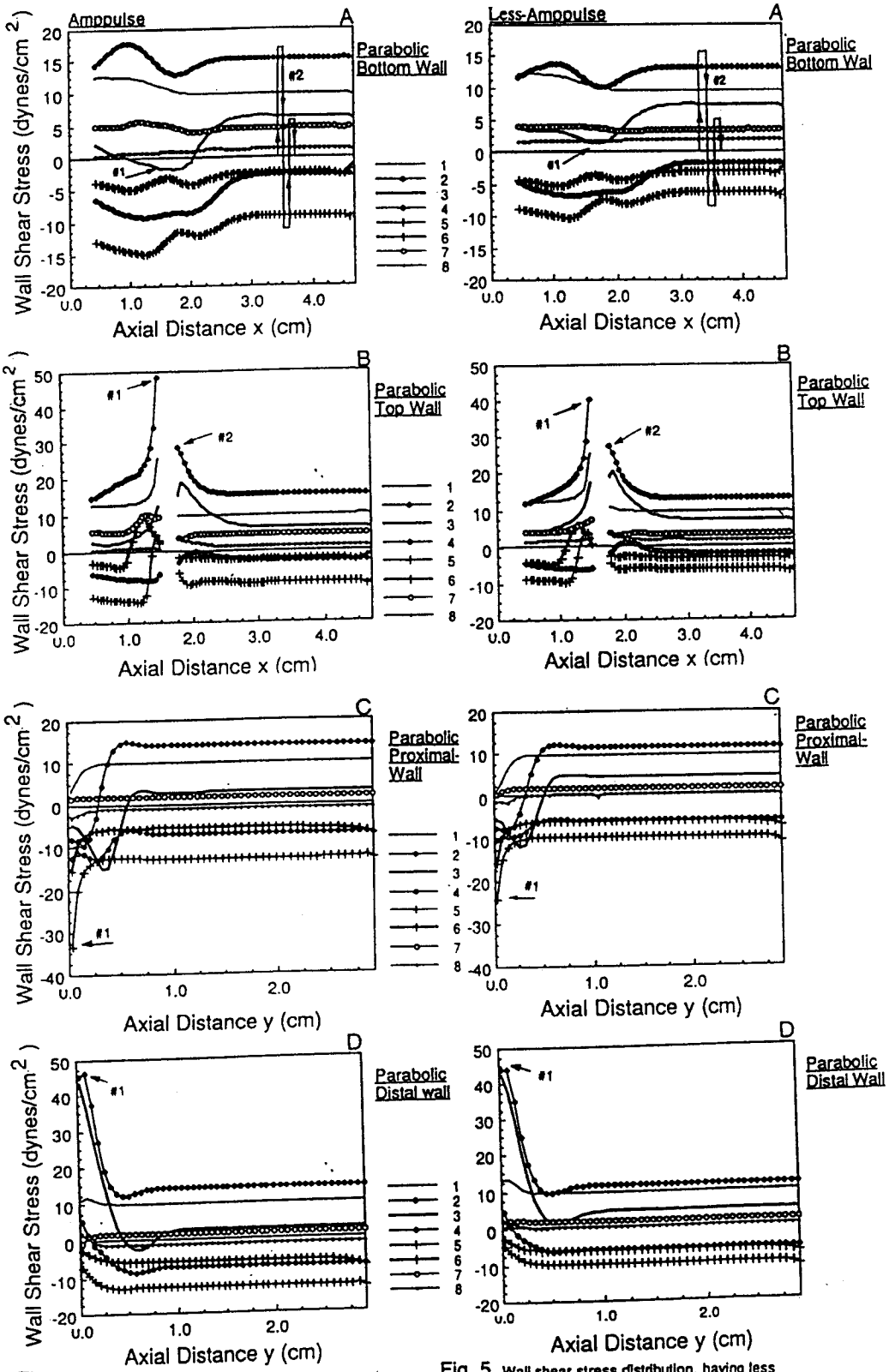


Fig. 4 Wall shear stress distribution, having ampoulse and parabolic inlet conditions, along the walls of main and branch lumens for different time steps of a pulse cycle.

Fig. 5 Wall shear stress distribution, having less ampoulse and parabolic inlet conditions, along the walls of main and branch lumens for different time steps of a pulse cycle.

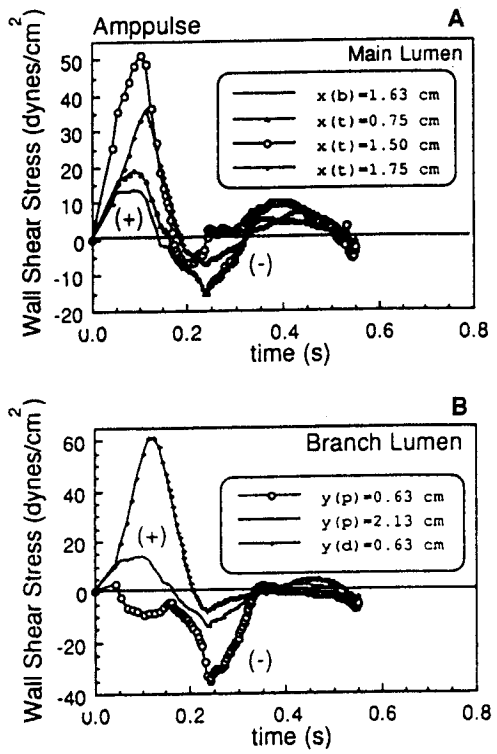


Fig. 6 Time histories of wall shear stress distributions at critical locations for amppulse flow. (p: proximal branch wall; d: distal branch wall; t: top main lumen wall; b: bottom main lumen wall)

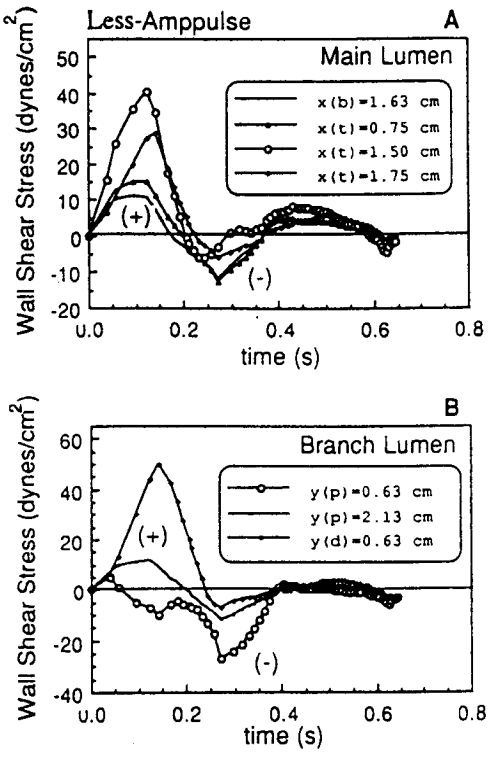


Fig. 7 Time histories of wall shear stress distributions at critical locations for less-amppulse flow. (p: proximal branch wall; d: distal branch wall; t: top main lumen wall; b: bottom main lumen wall)

in Fig. 6A). In comparison, for 'less-amppulse' circulation, at t = 0.122 s, the maximum shear stress of 40.3 dynes/cm$^2$ occurs at the same location (Fig. 7A) indicating a 21% reduction in peak shear stress value. For both type of circulations the bottom wall, opposite to the branch (x = 1.63 cm in Fig. 6A and 7A), experiences a 33% reduction in peak shear stress as compared to the normal value (x = 0.75 cm in Fig. 6A and 7A). In the main lumen a 17% reduction in the peak negative shear stress value is observed for 'less-amppulse' circulation (-12.72 dynes/cm$^2$ t = 0.273 s) as compared to 'amppulse' circulation (-15.3 dynes/cm$^2$ at t = 0.236 s).

For 'amppulse' circulation, at t = 0.117 s, the maximum wall shear stress of 60.9 dynes/cm$^2$ occurs at the distal branch wall apex (y = 0.63 cm in Fig. 6B). In comparison, for 'less-amppulse' circulation, at t = 0.142 s, the maximum shear stress of 49.9 dynes/cm$^2$ occurs at the same location (Fig. 7B) indicating a 18% reduction in peak shear stress value. In the branch lumen, a 23% reduction in the peak negative shear stress value at the proximal wall is observed for 'less-amppulse' circulation (-27.1 dynes/cm$^2$ at t = 0.273 s) as compared to 'amppulse' circulation (-35.2 dynes/cm$^2$ at t = 0.241 s).

## SUMMARY AND CONCLUSION

The repeated generation and shedding of the recirculating vortex near the branch resulted in an oscillatory wall shear stress and a shear rate that both depended on time and space. Sharp changes in the magnitude and the direction of the oscillatory wall shear stress values, as compared to a normal value, could create unfavorable physiological conditions that could lead to increasing damage to the arterial walls. These adverse physiological conditions, which were due to lower levels of oscillatory wall shear stress, were lipid deposition and depletion of oxygen transport. However, the mechanical damage to cells in arterial walls was due to higher levels of oscillatory wall shear stress. The combination of the above two could be responsible for the initiation and progression of atherosclerosis in branch regions.

Following distinctions were observed for 'amppulse' and 'less-amppulse' circulations:

i) A 'less-amppulse' circulation generated a more favorable hydrodynamic condition for the artery than an 'amppulse' circulation.

ii) A comparison between 'less-amppulse' and 'amppulse' circulations in a 90$^o$ branch region revealed that a lower magnitude and a shift in the oscillatory shear rate and shear stress were obtained for 'less-amppulse' circulation.

In sum, many adverse hydrodynamic conditions are observed for 'amppulse' circulation. The net result of 'amppulse' circulation is chronic mechanical damage to the vascular system, especially to the arterial walls; the amount of damage can be lessened by 'less-amppulse' circulation. 'Less-amppulse' circulation, an alteration of the pulsatile flow condition, may be achieved by pharmaceutical, chemical, or mechanical means; applied as treatment, such a process eventually may help to reduce the risk of arterial diseases, such as heart attack and stroke.

## REFERENCES


Baker, A.J. (1983) *Finite Element Computational Fluid Mechanics*, Hemisphere Publishing Corp.

Banerjee, R.K., Cho, Y.I. and Back, L. H. (1993) Numerical studies of non-Newtonian pulsed flow in a femoral branched vessel,*Advances in Fluid Engineering, ASME.*, [in press].

Cho, Y. I., Back, L. H., and Crawford, D. W. (1985) Experimental investigation of branch flow ratio, angle, and Reynolds number effects on the pressure and flow fields in arterial branch models, *ASME J. Biomech. Engrg.*, **107**, 257-267.

Risoe, C. and Wille, S. O. (1978) Blood velocity in human arteries measured by a bidirectional ultrasound doppler flowmeter, *Acta Physiol. Scand.*, **103**, 370-378.